

AN EXAMINATION OF FIM PERFORMANCE FOR A VARIETY OF WEATHER SCENARIOS

Edward J. Szoke^{1,2}, Stan Benjamin, John M. Brown, and Mike Fiorino
 NOAA Earth System Research Laboratory (ESRL), Boulder, Colorado

¹Collaboration with the Cooperative Institute for Research in the Atmosphere (CIRA), Fort Collins, Colorado

1. OVERVIEW OF THE FIM

Over the last year considerable effort has been made at the NOAA Earth System Research Laboratory (ESRL) to develop and test a new global model that includes unique features, such as use of the adaptive isentropic-sigma hybrid vertical coordinate successful with the RUC model, accurate finite-volume horizontal advection, and an icosahedral horizontal grid. The model has been named the FIM (<http://fim.noaa.gov>), for Flow-following finite-volume Icosahedral Model, and is currently being run twice per day at the Global Systems Division (GSD) of ESRL (see Benjamin et al. (2009, presentation in this conference), also Lee et al. 2007). Journal manuscripts describing the FIM in more detail are in preparation at ESRL.

There are several long-term goals for the FIM, including being a candidate for the North American Ensemble Forecast System (NAEFS). With this in mind, part of our assessment activities have included examination of model forecasts for various weather scenarios over different seasons. Comparisons have been made with the forecasts from other operational global models, including the Global Forecast System (GFS) model and the long-range model of the European Centre for Medium-Range Weather Forecasts (ECMWF). While a number of our cases focus on North American weather systems, we have also looked at forecasts from around the globe.

If the FIM model is to become part of the NAEFS it is important to gain an understanding of the reliability of the model forecasts and how they compare to those from other global models. Our efforts in this regard are summarized in this paper, with an overview of FIM performance followed by a look at a few representative cases. As noted on the FIM web page (fim.noaa.gov), the FIM model has been under continual development, and these cases shown below have been extracted from different points in this history (available on the web page).

²Corresponding author address: Ed Szoke, NOAA/ESRL/GSD,R/GSD, 325 Broadway, Boulder, CO 80305; e-mail: Edward.J.Szoke@noaa.gov

2. CHARACTERISTICS OF THE FIM

As noted, the acronym FIM indicates that the model uses a flow-following (i.e. quasi-Lagrangian) vertical coordinate, finite-volume numerics, and an icosahedral global grid. A more detailed description of the FIM can be found in the paper by Benjamin et al. (2009, this conference, paper 1A.4) The spacing of this icosahedral grid is unique in that it is basically the same at any point on the globe, rather than varying from pole to equator in a typical latitude/longitude grid point model. Figure 1 shows the FIM icosahedral grid with an overlaid image of potential temperature at the surface for a particular case.

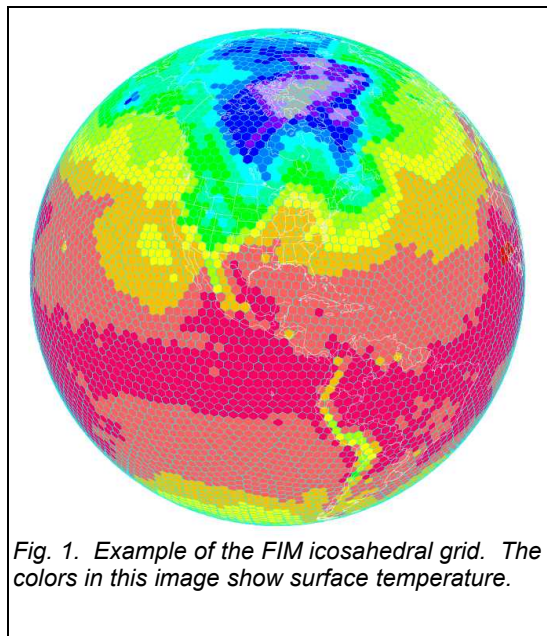


Fig. 1. Example of the FIM icosahedral grid. The colors in this image show surface temperature.

Currently the FIM is being run twice per day at NOAA/ESRL/GSD, at 1200 and 0000 UTC, out to 168 h. The current horizontal resolution for the FIM, as determined by the distance between the cell centers of the rhombi, 30.2 km, and is referred to as G8. The FIM uses an isentropic-sigma hybrid coordinate, similar to the Rapid Update Cycle (RUC) model. In November 2008 the vertical resolution was increased from 50 levels with a top at 2 hPa to 64 levels with a top at 0.5 hPa. More recently an improved land-use table has been used, and soon topography from the Weather Research and Forecasting Model (WRF), rather

than the topography from the GFS, will be incorporated. The FIM is initialized using the GFS analysis.

Graphical forecast output is posted at 3-h intervals on the FIM web site at <http://fim.noaa.gov/>. Output is also available on the Advanced Weather Interactive Processing System (AWIPS) workstation at GSD, and on the Advanced Linux Prototype System (ALPS) workstations at both GSD and the co-located National Weather Service (NWS) Boulder Weather Forecast Office (WFO).

3. OVERVIEW OF FIM PERFORMANCE

In addition to examining individual cases of model performance for the FIM and comparing it with other models on a case-by-case basis, we initially began examining FIM's performance in the spring and summer of 2008 by a more systematic look at global forecasts of 300 mb level jets (defined as wind maximum greater than or equal to 120 kts) and mean sea level pressure (MSLP) centers (for both high and low pressure centers defined by a closed contour at an 8 mb interval).

These initial studies determined the following characteristics of the FIM forecasts for the summer months (Northern Hemisphere (NH)) of 2008 (Southern Hemisphere (SH) winter):

- Initial analyses for both MSLP and 300-mb jets were nearly identical between the FIM and GFS. While expected given that the GFS is used for the FIM initial conditions, this confirmed there were no issues in interpolating to the coordinate system used in the FIM.
- Small differences in wind speed within the jet maxima were found by 24 h, averaging out to a slight underprediction for the FIM and slight overprediction for the GFS in the NH. Both models overpredicted the jet maxima strength in the SH, moreso in the GFS (1.1 vs. 5.8 kts).
- By five- and seven-day forecasts the FIM tended to underpredict the jet maxima, especially in the NH, while the GFS had a modest underprediction in the NH and overprediction in the SH.
- Generally the same jet maxima could be identified in both models, although there were some location differences in the longer-range forecasts.
- We did not determine that there were any systematic differences between the MSLP forecasts based on comparison of high and low pressure centers.

During the summer/fall season of 2008 we also examined FIM forecasts of tropical storms and hurricanes. The tropical season of 2008 was quite active and a number of storms were studied. Assessment activities are still underway, and only

a brief summary is given here. The FIM was also run at G9 resolution (~15 km horizontal resolution) at the Texas Advanced Computing Center (TACC) for most of the storms.

The FIM had no trouble developing tropical storms, and did not necessarily develop the same initial storms that were found in the GFS or ECMWF. For those storms that were similar, in general, the strength of the storm was similar to the GFS, while the ECMWF tended to both initialize and maintain stronger systems than either the FIM or GFS, though this was not always the case. The tracks were not always similar between the three models. Overall it appeared that the forecasts from the FIM provided a reasonable spread to the predictions from the other global models.

An example of a forecast from a particularly active period is shown in Fig. 2, with the accompanying verifying analysis for the five-day forecast in Fig. 3. At the initial time of the forecast, 1200 UTC on 28 August (Fig. 4), Gustav (yellow oval in the figures) was a tropical storm, after weakening from a Category 1 hurricane when it passed over Haiti, and Hanna had just become a tropical storm. The system that would become Ike, in the red oval, was still just a tropical wave that was being monitored as it emerged off the African coast.

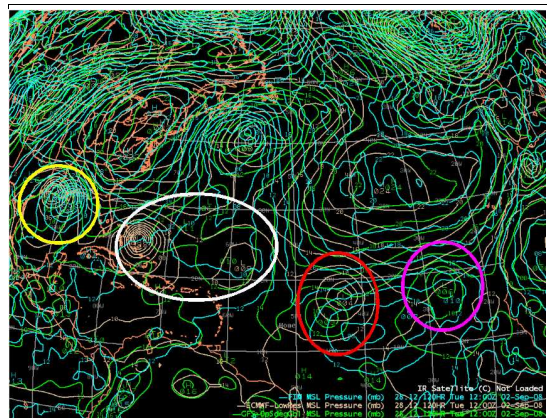


Fig. 2. MSLP 120-h forecasts from the 1200 UTC 28 August 08 runs of the FIM, ECMWF, and GFS, valid at 1200 UTC on 2 September. The 4 predicted storms are highlighted: Gustav (yellow oval), Hanna (white), Ike (red), and Josephine (magenta).

Examination of the 120-h forecasts in Fig. 2 shows differences among the forecasts for the four storms, with the FIM providing reasonable-looking diversity in the predictions. At the verification time (1200 UTC/2 Sep, Fig. 3) Gustav was rapidly weakening in west-central Louisiana, after making landfall along the central Louisiana coast near Category 3 strength. The forecast from the FIM is very close in position to that from the ECMWF, and

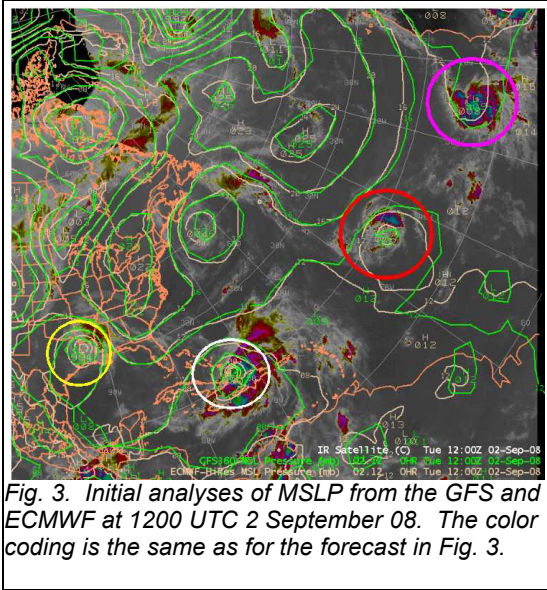


Fig. 3. Initial analyses of MSLP from the GFS and ECMWF at 1200 UTC 2 September 08. The color coding is the same as for the forecast in Fig. 3.

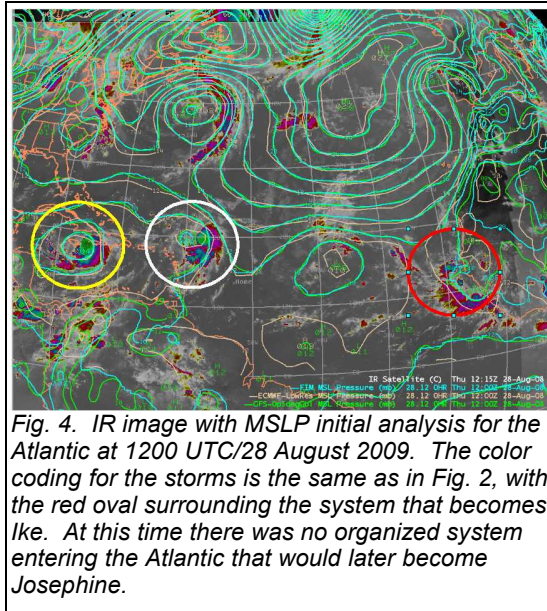


Fig. 4. IR image with MSLP initial analysis for the Atlantic at 1200 UTC/28 August 2009. The color coding for the storms is the same as in Fig. 2, with the red oval surrounding the system that becomes Ike. At this time there was no organized system entering the Atlantic that would later become Josephine.

both are closer to the verifying position than the GFS. Hanna (white oval), a 987 mb tropical storm at verification time, had the most widely varying forecasts. The ECMWF came closest, with a significant storm that was a little faster moving westward than observed. This was far better than the much weaker storm that was predicted by both the FIM and the GFS. Farther to the east, Ike had become a tropical storm at ~1003-mb strength. For this storm the FIM was slower and weaker than the GFS and ECMWF. Examination of other longer-range forecasts for Ike actually showed that the FIM and GFS had good forecasts showing the development of a system, in fact earlier than seen in the ECMWF. Josephine was about to be named a tropical storm at ~1006 mb, and the forecast from the FIM was similar to the ECMWF, which were both somewhat weaker than the GFS.

A final example from last year's Atlantic hurricane season is shown in Fig. 5, which is a comparison of forecast tracks for hurricane Ike from the FIM8 and FIM9 with other models routinely used at the Tropical Prediction Center. The forecasts in Fig. 5 were initialized on 0000 UTC/10 September, and landfall occurred near 1200 UTC/13 September near Galveston, which is quite close to the forecast track from the FIM9, the higher-resolution version of the FIM. The forecast tracks for the other models are all grouped to the south of where Ike made landfall, although the FIM8 track is at the northern edge of this envelope of tracks. Although this example shows a distinctly better forecast track for the higher-resolution FIM, this was not always the case when we examined other initialization times. As an example, forecast tracks from the set of models initialized at 0000 UTC/8 September for Ike are shown in Fig. 6. For this time, the envelope of most model forecast tracks was too far to the east and north of landfall. This time the FIM8, the lower-grid resolution FIM, had the best track, and was distinctly different from the others.

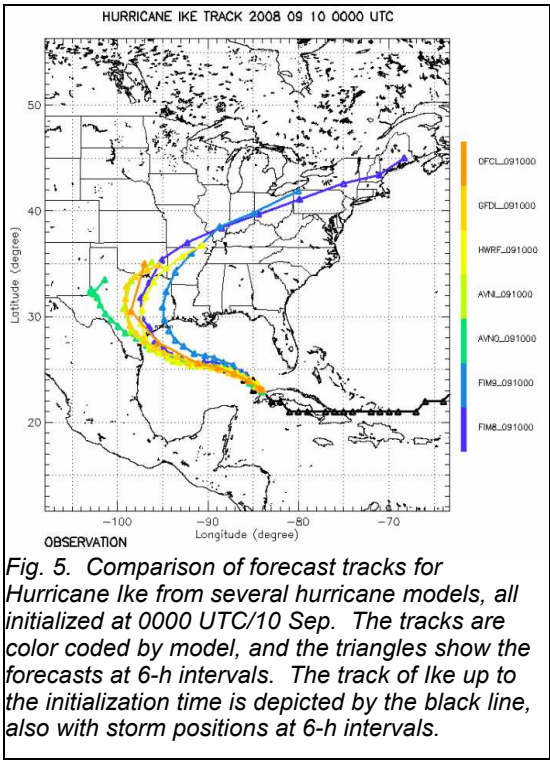
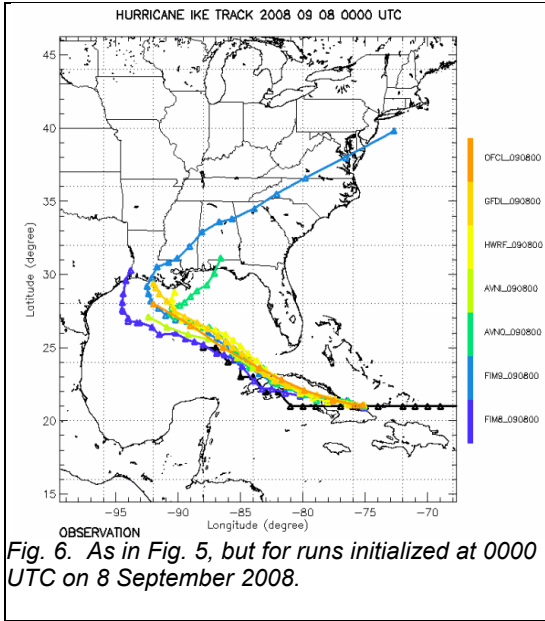


Fig. 5. Comparison of forecast tracks for Hurricane Ike from several hurricane models, all initialized at 0000 UTC/10 Sep. The tracks are color coded by model, and the triangles show the forecasts at 6-h intervals. The track of Ike up to the initialization time is depicted by the black line, also with storm positions at 6-h intervals.

For other initialization times, the FIM8 and FIM9 forecast tracks tended to lie within the general envelope of most of the other model tracks. Overall, for Ike as well as other storms studied during the last tropical season, the forecasts of tracks from the FIM runs generally represented a reasonable contribution to a multi-model ensemble hurricane forecast.

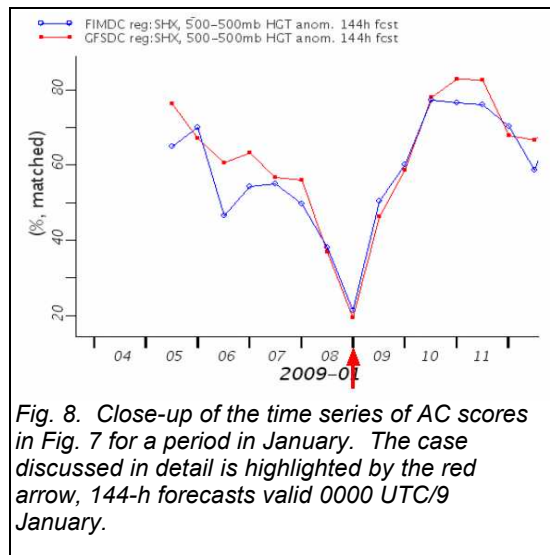
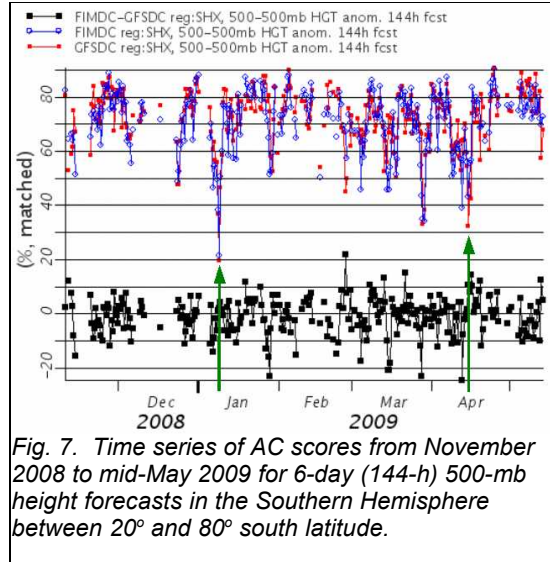


4. CASES

In this section we will examine a few cases that demonstrate some of the characteristics of the FIM8 (hereafter simply FIM) forecasts, and how they compare to other global models and to the verifying weather. A number of cases have been examined over the past 12 to 18 months, and these represent a very limited sample. As noted earlier, objective verification is also being done for FIM forecasts, including point comparison with rawinsonde data. Anomaly correlation (AC) scores are being calculated for height and u and v wind components, similar to what is done at NOAA's National Center for Environmental Prediction (NCEP). Computations of the anomaly correlation score for a user-selected level can be made using the interactive GSD web site at <http://ruc.noaa.gov/stats/anom/beta/>. We used the 500-mb AC scores to identify some of the cases that were selected. Others were based on noting subjectively when the model forecasts tended to diverge from one another. Generally, we focused on longer-range forecasts of five to seven days out, though not exclusively.

4.1 Southern Hemisphere AC “dropout” case

A very distinct and relatively short-lived period of extremely poor longer-range model performance in the Southern Hemisphere was easily identified in the AC time series. The worst forecast had a very distinct low AC score, known as a “dropout”. It is highlighted by the green arrow in early January in the time series in Fig. 7, and this is the lowest score in the 5+ month time series. A close-up of the time series in Fig. 8 reveals that the single initialization time of 0000 UTC/2 January led to the most notably poor forecast, the 144-h forecast



valid on 0000 UTC/9 January. Next we will examine the details of this particular forecast to determine the nature of the poor performance.

The offending forecasts from the GFS and FIM are shown in Fig. 9 along with the FIM analysis for the verifying time of 0000 UTC on 9 January. Areas where the forecasts differed most from the analysis are highlighted by the different colored ovals, with the exception of the white oval east of Australia. This highlighted area is actually a tropical storm that was not present as an organized storm at the initialization time, but nonetheless was forecast quite well by both the FIM and GFS six days later. The wave southeast of South America has a similar forecast in both the GFS and FIM and is a broader wave in the forecast than in the analysis. But the most egregious forecast errors occur with the two systems to the southwest and south of Africa (red and magenta ovals).

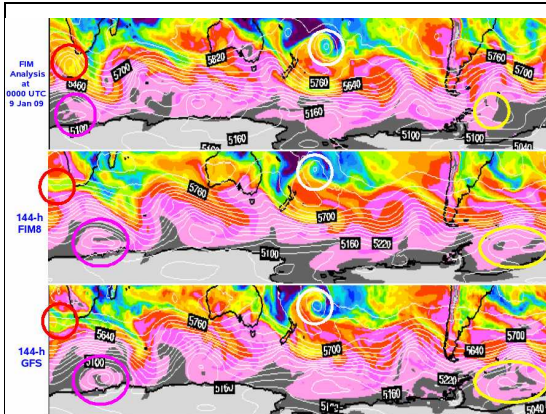


Fig. 9. Set of SH 144-h 500-mb forecasts from the FIM (middle image) and GFS (bottom image) valid 0000 UTC/9 January, with the verifying analysis from the FIM (top). Interesting areas are highlighted by the various colored ovals. The image is total precipitable water.

There are two separate systems that end up being considerably off in the forecasts and that appear to be the main source of the large AC error. One is a system that moves across the Atlantic and ends up off the southwest tip of South Africa by the verification time of 0000 UTC/9 January. The other is a broader and less intense system that moves northward from near Antarctica and ends up to the south-southeast of the southern tip of Africa. The models pick up on this second system but both have timing errors by 144 h such that the shortwave ridge/trough pattern is out of phase, leading to substantial height errors near this system.

The other system that moves across the Atlantic becomes a very intense storm during the time of the forecast cycle, then has begun to fill before 9 January. A series of IR images showing the development of the storm from the initialization time of the model runs at 0000 UTC/3 January through the 144-h forecast time of 0000 UTC/9 Jan is in Fig. 10. At the time the models are initialized, a system is emerging off the east coast of South America. Both the GFS and FIM appear to pick up on a system in this area, as seen in the comparison of the two analyses in Fig. 11. In fact, at 48-h into the forecast the wave still appears to be predicted fairly well by both the GFS and FIM (Fig. 12). Thereafter, however, neither model is able to capture the rapid cyclogenesis that occurs, as seen in the satellite imagery. By 72-h out (Fig. 13) the intensity of the system seen in the analysis is not captured in either forecast.

The valid time of 0000 UTC/6 January for the 72-h forecast is the same time as one of the satellite images in Fig. 10, which nicely shows the system wrapping up, in agreement with the analysis at this time shown in Fig. 13. The forecasts after 72-h get worse, as the system

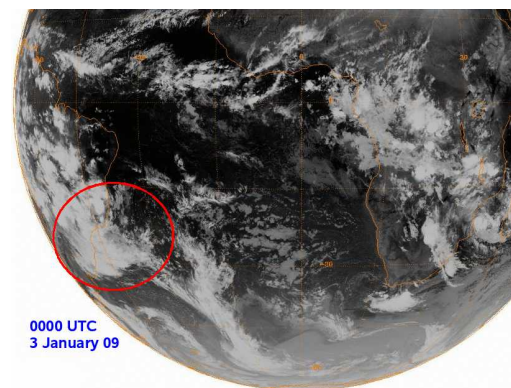
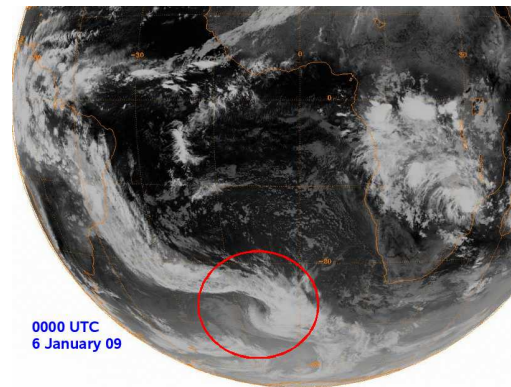
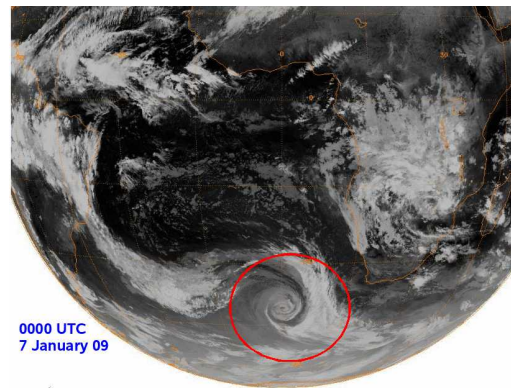
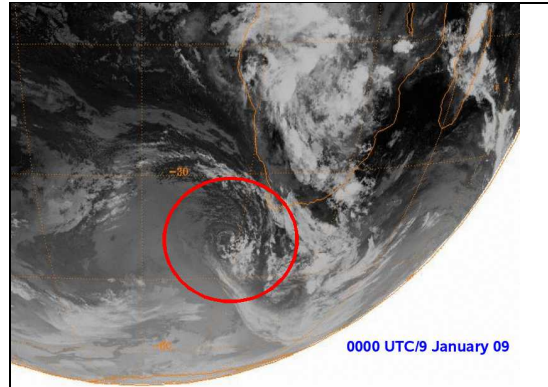


Fig. 10. Series of IR images with the storm of interest circled in red.

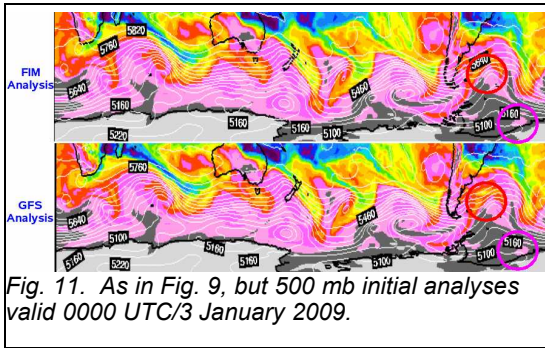


Fig. 11. As in Fig. 9, but 500 mb initial analyses valid 0000 UTC/3 January 2009.

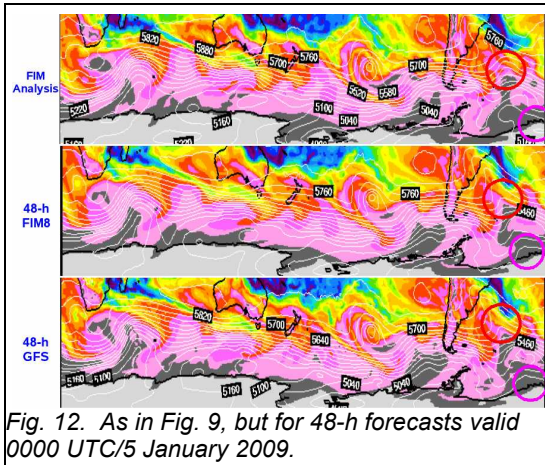


Fig. 12. As in Fig. 9, but for 48-h forecasts valid 0000 UTC/5 January 2009.

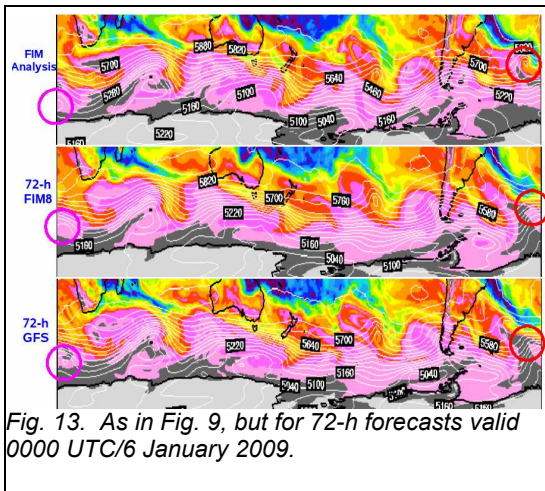


Fig. 13. As in Fig. 9, but for 72-h forecasts valid 0000 UTC/6 January 2009.

weakens slightly in the model forecasts, when in fact it strengthens for an additional 24 to 36-h. The model performance for this event did improve fairly rapidly with subsequent runs, as seen in the AC time series in Fig. 8, as models were better able to capture the cyclogenesis, and had better timing with the other system.

4.2 Mid-May 09: Diversity of the FIM forecasts.

One of the advantages to having an addition to the NAEFS would be for a model to have forecasts that augment the forecast spread in a meteorological, reasonable manner, and not

necessarily follow the forecasts from other models exactly. Here we examine a series of recent longer-range (7 day) forecasts for a modest weather system during a period of relatively zonal flow that occurred in early to mid-May 2009. Differences were noted in the speed and strength of systems entering the western Continental United States (CONUS). The purpose of examining these forecasts was to determine if the FIM followed a particular model (GFS or ECMWF) or showed a trend of any sort.

The first forecast in this series is shown in Fig. 14. The top figure shows 168-h 500-mb height forecasts from the 1200 UTC/5 May 2009 runs of the GFS, FIM and ECMWF. The analysis for the valid time of 1200 UTC/12 May 2009 is shown in the bottom of Fig. 14. Focusing on the trough entering the western CONUS, the GFS and FIM forecasts have similar forecasts with one main trough heading into the Pacific Northwest, while the ECMWF has split this trough into two waves, the stronger one still off the coast and north of the

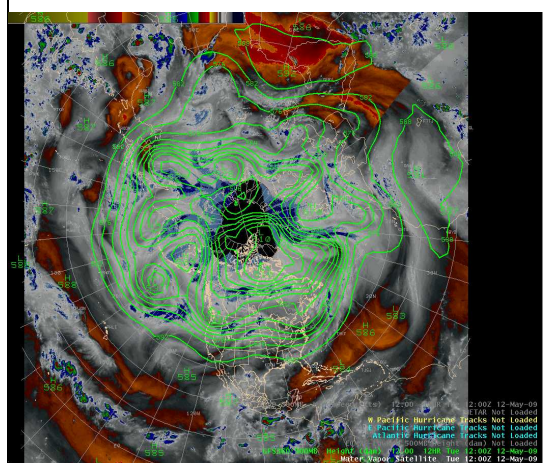
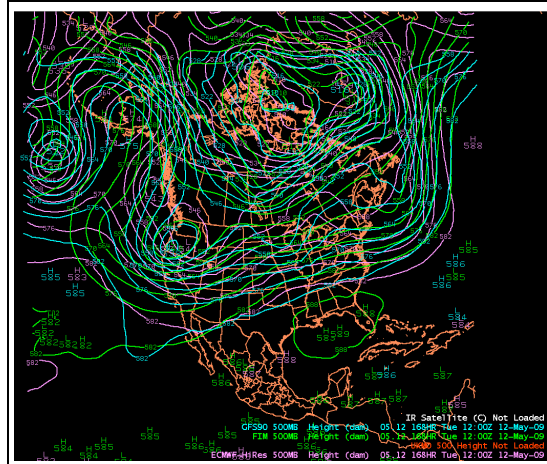


Fig. 14. Comparison of 168-h 500-mb height forecasts from the ECMWF, GFS and FIM initialized at 1200 UTC/5 May 2009 (top). Bottom image shows the 500-mb analysis with satellite water vapor/IR imagery for the verification time of 1200 UTC/12 May.

trough forecast by the GFS and FIM. The verifying analysis supports more of a single trough solution similar to the FIM and GFS. Although the FIM and GFS have the best forecast for the western trough, downstream the GFS has a distinct shortwave trough over Minnesota. This is not found in the other models, and in fact a shortwave ridge actually verifies in this location.

The next set of 168-h forecasts shown in Fig. 15 are from the runs initialized 12-h later, at 0000 UTC/6 May. This time the two similar runs in the forecast of the western CONUS trough are the FIM and the ECMWF, while the GFS is deeper than the other two models. The verifying analysis in Fig. 15 indicates that for this time a shallower trough, as in the FIM and ECMWF forecast, verifies best.

The final forecast time shown for this sequence is from the set of 168-h forecasts initialized 12-h later, at 1200 UTC on 13 May, with the forecasts shown in Fig. 16 along with the verifying analysis. For this forecast time, each model has a somewhat different forecast, both for the wave undercutting the upper-level ridge off the West Coast and in the details in the western CONUS. In the western CONUS the faster ECMWF, and to a lesser extent

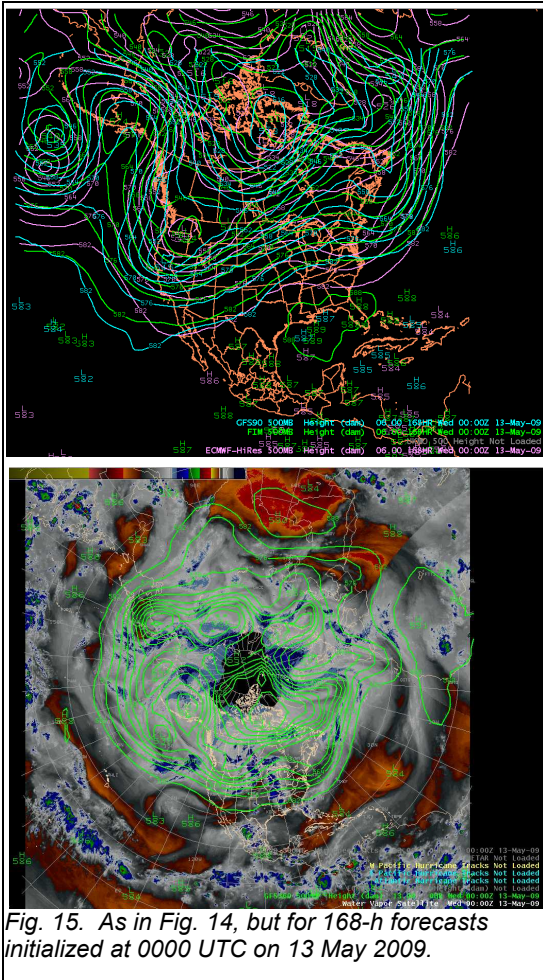


Fig. 15. As in Fig. 14, but for 168-h forecasts initialized at 0000 UTC on 13 May 2009.

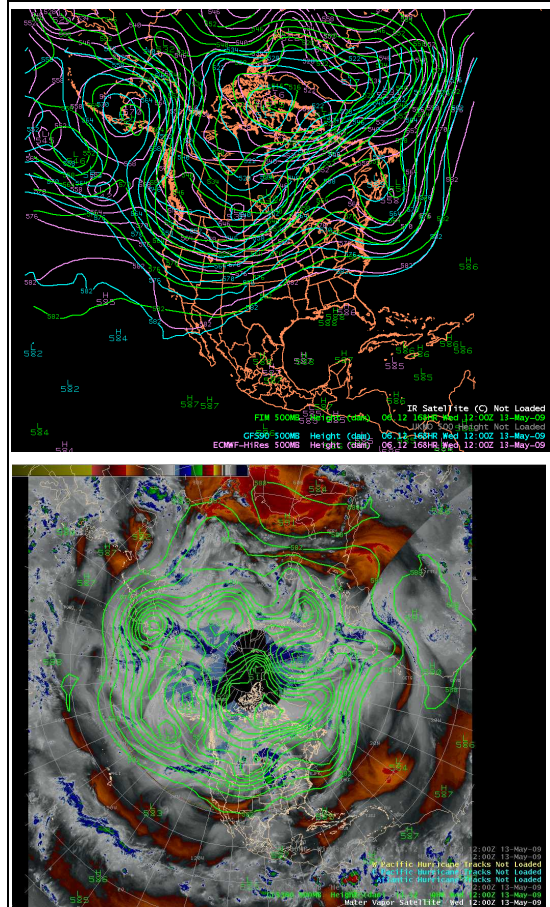


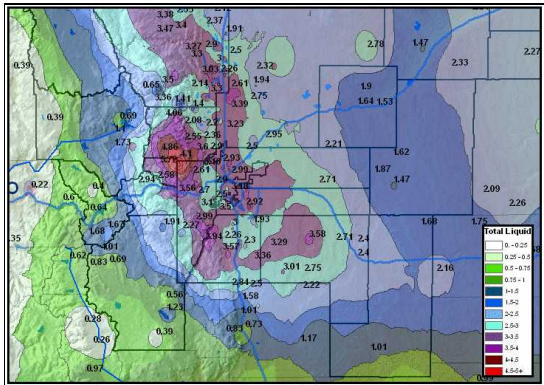
Fig. 16. As in Fig. 14, but for 168-h forecasts initialized at 1200 UTC on 13 May 2009.

the GFS, verify better than the FIM. Off the West Coast, the simpler one-wave solution found in the FIM and GFS verifies better than the ECMWF.

The main point illustrated by this set of three consecutive 168-h forecasts is that the FIM solution did not favor either the GFS or ECMWF, being similar to each of these models at different times. The FIM also sometimes offered a forecast that varied from either model, but was a reasonable-looking longer-range forecast for this situation.

4.3 The “Big One”: huge Colorado mountain/foothill snowstorm of 17-18 April 09.

The last case shown will examine some of the forecasts from the various models for a significant event in Colorado and surrounding areas in mid-April 2009. A slow-moving upper-level closed low produced several inches of precipitation over much of Colorado, with the precipitation falling as heavy snow along the Front Range and nearby mountain areas. The precipitation was widespread, as shown in the summary of the storm in Fig. 17, which was compiled by the Boulder National Weather Service (NWS) Weather Forecast Office

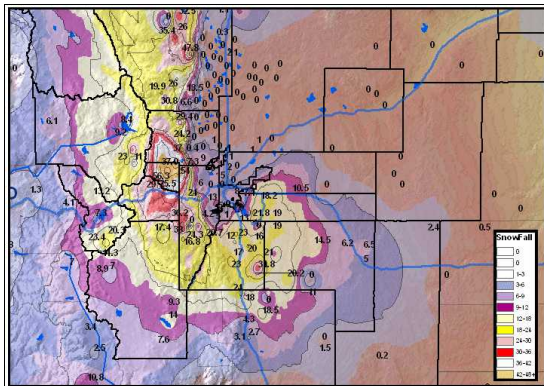


The above image depicts total rainfall amounts across Northeast Colorado. As the map highlights, the highest liquid precipitation amounts were found in the foothills west of Denver. Most areas across metro Denver received between 2.5 and 3.5 inches of liquid precipitation.

Top 5 reporting Liquid Precipitation Amounts

Location	Rainfall Total	County
3 SE Pinecliffe	5.72	Gilpin
Foxfield 2.3	4.51	Arapahoe
Nederland 5.8E	4.86	Boulder
Boulder 3.5 S	4.47	Boulder
Boulder 2.7 S	4.37	Boulder

Fig. 17. Precipitation amounts for Northeast Colorado (inches) overlaid on a topography image for the period 16-19 April 2009. The top five precipitation amounts are listed in the table.



The above image depicts total snowfall amounts across Northeast Colorado. As the map highlights, the highest snowfall amounts were found in the foothills west of Denver.

Top 5 reporting Snowfall Amounts

Location	Snowfall Total	County
3 S Rollinsville	56.3	Gilpin
3 SE Pinecliffe	54	Jefferson
1 E Buckhorn Mtn	47.8	Larimer
Aspen Springs	43.4	Gilpin
2 ESE Pinecliffe	40.3	Gilpin

Fig. 18. As in Fig. 17, but for snowfall (inches).

(WFO). Many areas received over 2 inches of precipitation, with foothill locations closer to 5 inches (peak amount was 5.72 inches in the foothills). Final snowfall amounts (Fig. 18) in the foothills exceeded four feet in some areas, making this the biggest event since the great March 2003 storm (Szoke et al. 2004). Snowfall was closely tied to elevation, with the snow level near 5500 feet.

Here we will concentrate on some of the longer-range (seven days or less) forecasts for the event. There were significant problems predicting this event, and large differences between the more progressive GFS and the ECMWF, which consistently held the system back in the Rockies. The differences were quite extreme in the 8- to 10-day range, and the same issues carried over into forecasts out to about five days. Interestingly, some of the same forecast discrepancies were

found in the long and even medium range forecasts for the great March 2003 storm, which was a similar event.

Since the FIM forecasts end at seven days (168 h), we begin our comparison with the longer-range forecasts seven days out. The AC scores for the 1200 UTC 168-h forecasts for the Northern Hemisphere (Fig. 19) show a distinct drop for the forecasts valid at 1200 UTC on 17 April 2009. The 500-mb analysis for this time is shown in Fig. 20, and indicates an upper-level low in an ideal position to provide significant upslope-forced precipitation for Colorado. The slow-moving nature of this event and high moisture levels made this a very significant spring storm.

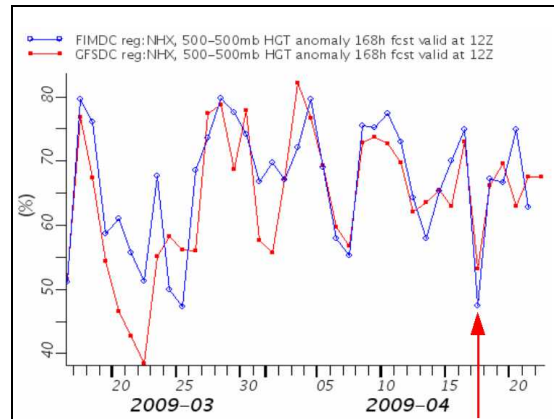


Fig. 19. AC scores for 168-h 500-mb forecasts from the 1200 UTC runs of the GFS (red) and FIM (blue) for the Northern Hemisphere. The forecasts valid at 1200 UTC on 17 April 2009 are highlighted by the red arrow.

The first set of forecast comparisons are for 168-h forecasts valid at the time in Fig. 20, 1200 UTC on 17 April, and are representative of the long-range forecast problems with this event. The FIM forecast is shown in Fig. 21, and is clearly much too far to the north and much more progressive with the trough. The system forecast by the FIM would result in little if any precipitation

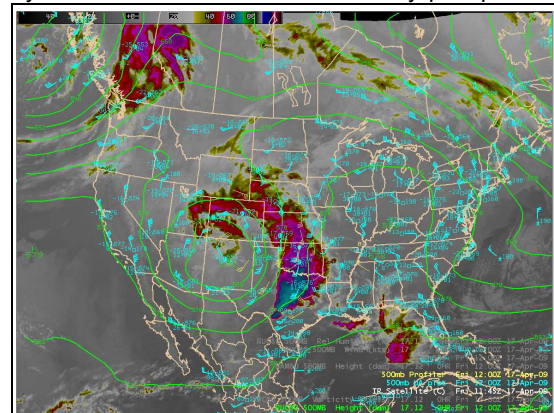


Fig. 20. 500-mb height analysis and plot overlaid with an IR satellite image for 1200 UTC/17 April.

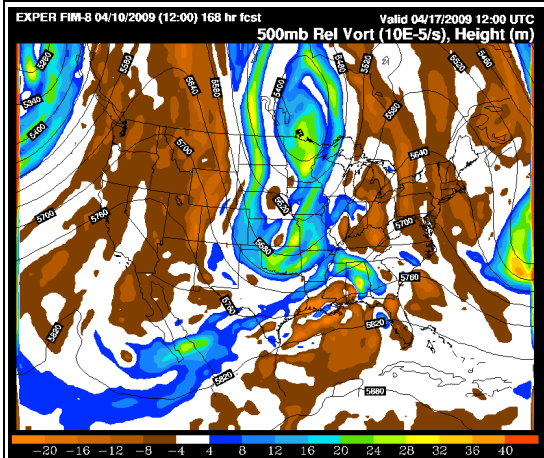


Fig. 21. FIM 168-h 500-mb height and vorticity (image) forecast from the 1200 UTC/10 April run, valid 1200 UTC/17 April 2009.

for Colorado. The GFS (Fig. 22) forecast is a little farther south (earlier forecasts were as far north as the FIM), but not much better in that basically downslope flow and little precipitation were predicted for Colorado. The ECMWF (Fig. 23) is

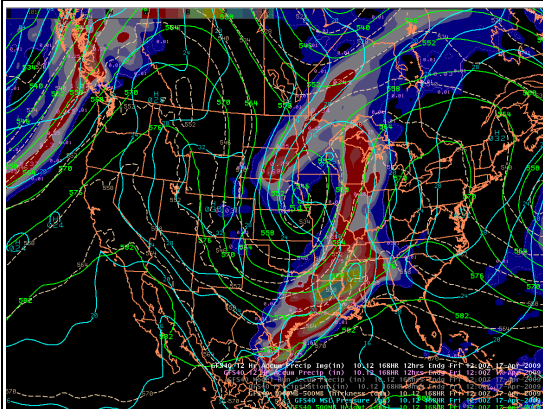


Fig. 22. As in Fig. 21, but for the GFS forecast. The 500-mb height is shown by the solid yellow contours. Also shown is MSLP (cyan solid lines, in mb), 1000-500 mb thickness (tan dashed lines, in dm), and 12-h precipitation ending at 1200 UTC (blue dotted line and image, in inches).

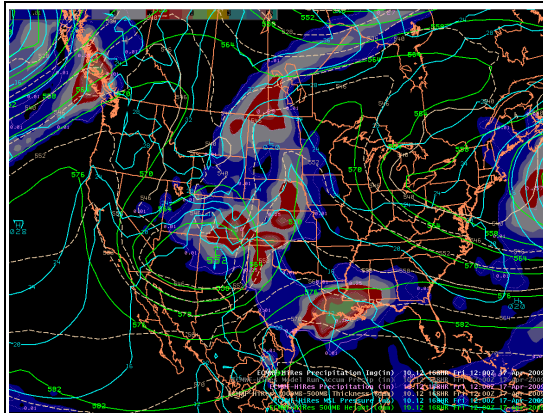


Fig. 23. As in Fig. 22, but for the ECMWF.

much better, and fairly close to the verifying analysis. This ECMWF was consistently superior to the GFS (and later the FIM) for this event before the forecasts came into better agreement about five days out.

The forecasts from the GFS and FIM became more consistent and closer to the ECMWF and reality 24-h later, with the runs initialized on 1200 UTC/11 April. In fact, the FIM tended to bring the upper-level low southward earlier than the GFS. This can be seen by the comparison of the FIM and GFS 144-h forecasts from the 1200 UTC runs on 11 April in Figs. 24 and 25, with the valid time (Fig. 20) the same as for the previous forecasts. Interestingly, the ECMWF forecast, shown in Fig. 26, predicted a more north-south elongated upper-level low in this run cycle, and is not as good (or consistent) as most of its earlier forecasts.

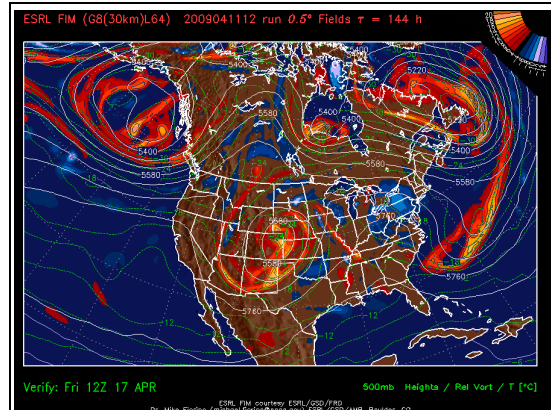


Fig. 24. 144-h 500-mb height (contours) and vorticity (image) forecasts from the 1200 UTC 11 April run of the FIM, valid at 1200 UTC on 17 April.

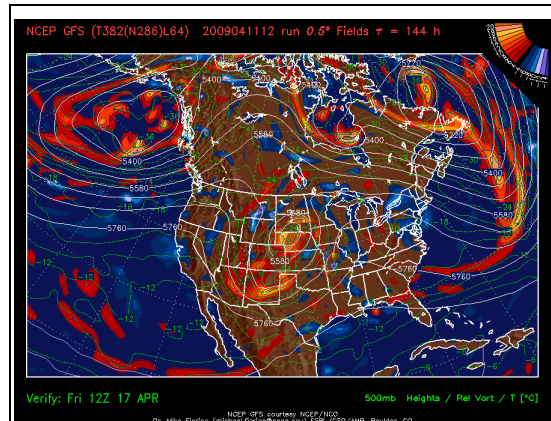


Fig. 25. As in Fig. 24, except for the GFS forecast.

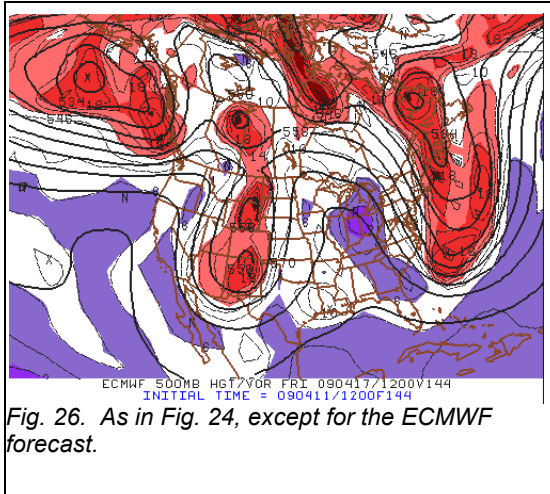


Fig. 26. As in Fig. 24, except for the ECMWF forecast.

model., Preprints, *22nd Conference on Weather Analysis and Forecasting/18th Conference on Numerical Weather Prediction*, Park City, UT, Amer. Meteor. Soc.

Szoke, E. J., B. L. Shaw, P. Schultz, and D. Barjenbruch, 2004: Performance of various operational and experimental numerical forecasts for the March 2003 Colorado snowstorm. *20th Conference on Weather Analysis and Forecasting/16th Conference on Numerical Weather Prediction*, Seattle, WA, Amer. Meteor. Soc., Paper 10.3a.

5. SUMMARY AND CONCLUSIONS

Although still a “young” numerical model that continues to undergo improvements as well as some debugging of errors, the performance of the FIM over the last year or so, examined here for a variety of situations, is seen to be within the envelope of solutions provided by other operational models. While currently initialized with the GFS, the FIM does not necessarily follow the GFS forecasts. The spread of the FIM solutions compared to other models suggests that the FIM could potentially be a useful addition to the NAEFS.

As noted, improvements continue to be made with the FIM, and we will again be closely following the tropical performance of the G8 and hopefully G9 FIM during the upcoming Northern Hemisphere hurricane season. The current objective scoring will continue, as well as additional studies of varying weather scenarios in the future.

5. ACKNOWLEDGMENTS

We thank Brian Jamison of GSD for an internal scientific review and Annie Reiser of GSD for a technical review.

6. REFERENCES

- Benjamin, S., J. Lee, R. Bleck, J. W. Bao, A. E. MacDonald, J. M. Brown, T. Henderson, J. Middlecoff, C. Harrop, N. Wang, W. Moninger, G. Grell, S. Sahn, and B. Jamison, 2009: Real-time testing and description of the FIM global model. *23rd Conference on Weather Analysis and Forecasting/19th Conference on Numerical Weather Prediction*, Omaha, NE, Amer. Meteor. Soc., Paper 1A.4.
- Lee, J.L., R. Bleck, A.E. MacDonald, J.W. Bao, S. Benjamin, J. Middlecoff, N. Wang, J. Brown. FIM: A vertically flow-following, finite-volume icosahedral